~~Indices~~ Metrics of the Hadley circulation strength and associated circulation trends

Matic Pikovnik[1], Žiga Zaplotnik[1], Lina Boljka[2], and Nedjeljka Žagar[3]

[1]Faculty of Mathematics and Physics, University of Ljubljana, Ljubljana, 1000, Slovenia
[2]Geophysical Institute, University of Bergen and Bjerknes Centre for Climate Research, Bergen, 5020, Norway
[3]Meteorological Institute, Center for Earth System Research and Sustainability, Universität Hamburg, Hamburg, 20146, Germany

Correspondence: Žiga Zaplotnik (ziga.zaplotnik@fmf.uni-lj.si)

Abstract. This study compares ~~the trends of~~ trends of the Hadley cell (HC) strength using different ~~HC measures~~ metrics applied to the ECMWF ERA5 and ERA-Interim reanalyses in the period 1979-2018. The HC strength is commonly evaluated by ~~indices~~ metrics derived from the mass-weighted zonal-mean stream function. Other ~~measures include the velocity potential and~~ metrics include the upper-tropospheric velocity potential, the vertical velocity ~~. Six known measures~~ in the mid-troposphere, and the water vapour transport in the lower troposphere. Seven known metrics of the HC strength are here complemented by a ~~measure of the average~~ metric of the spatially-averaged HC strength, obtained by averaging the stream function in the latitude-pressure (φ-p) plane, and by the total energy of ~~unbalanced~~ zonal-mean unbalanced circulation in the normal-mode function decomposition. It is shown that ~~measures of the HC strength~~metrics, which rely on ~~point~~ single-point values in the φ-p plane, produce unreliable ~~long-term~~ 40-year trends of both the northern and southern HCs, especially in ERA-Interim; magnitudes and even the signs of the trends depend on the choice of ~~HC strength measure~~the HC strength metric. The two new ~~measures~~ metrics alleviate the vertical and meridional inhomogeneities of the trends in the HC strength. In both reanalyses, there is a positive trend in the total energy of zonal-mean unbalanced circulation. The ~~average HC strength measure~~ spatially-averaged HC strength metric also shows a positive trend in ERA5 in both hemispheres, while the trend in ERA-Interim is insignificant.

1 Introduction

The Hadley circulation is a thermally forced overturning circulation, consisting of two symmetrical cells, which span between the tropics and the subtropics. Each cell consists of the ascending branch in the deep tropics, which is associated with enhanced precipitation, poleward upper-tropospheric flow, and the descending motion in the subtropics that suppresses rainfall~~, and~~ . The cell is completed by a frictional return flow in the lower troposphere. Therefore, potential changes of the Hadley cells (HCs), either to their strength or their meridional extent, will have a profound impact on the global hydrological cycle (**??**) and the biosphere, particularly in the subtropics. For example, the subsidence region has already become drier, partly because of the enhanced descending motion, in line with the satellite observations of upper tropospheric humidity and total water vapor (**?**).

~~A number of~~ Several studies of the HC strength using reanalyses suggested strengthening of both the northern ~~HC~~ Hadley cell (NHC) and southern ~~HC~~ Hadley cell (SHC) in the recent decades. However, the reported magnitude and uncertainty of

the trends differ (**?????**). This is, alongside ~~different reanalyses (with~~ differences among reanalysis datasets (e.g. different resolutions ~~) and~~ and use of observations), study periods used and multidecadal variability (**??**, in review), partly due to a variety of metrics that have been used to define the HC strength. For example, the strength of the overall Hadley circulation can be evaluated using the velocity potential in the upper troposphere, ~~e.g. at 200 hPa, as~~ where the meridional divergent flow in the upper branch of the HC is strongest~~there~~, which is associated with the maximal upward motions in the layer beneath (**?**). The Hadley circulation strength can also be defined by the ~~minimum pressure velocity ω~~ maximum ascent at some predefined mid-tropospheric level (**?**). Both ~~measures~~ metrics describe the properties of the ascending branch of the Hadley circulation.

The majority of ~~the~~ studies describe the HC by the mass-weighted zonal-mean stream function ψ in the latitude-pressure (φ-p) plane (**?**). The ψ function is computed by the vertical integration of the zonal-mean meridional wind as

$$\psi(\varphi,p) = \frac{2\pi R\cos\varphi}{g}\int_0^p [v](\varphi,p')\mathrm{d}p', \tag{1}$$

where $[v]$ is the zonal- and annual/~~seasonal/monthly-mean~~ seasonal-mean meridional wind, R is Earth's radius, g is gravity, φ is latitude, and p is pressure. Several ~~indices~~ metrics of the HC strength based on ~~point~~ single-point values (maxima or minima) of $\psi(\varphi,p)$ have been used:

1. the maximum (minimum) values of ψ in the φ-p plane (e.g. **???**);
2. the maximum (minimum) value of ψ at some selected pressure level, e.g. 500 hPa ~~(e.g. ????)~~(e.g. **?????**);
3. the vertical average of the maxima (minima) of ψ at different pressure levels in the troposphere (e.g. in the layer 200 hPa - 900 hPa, as in **?**).

~~**?** is also the only study that addresses the vertical inhomogeneity of the HC strength and its trends.~~

~~While~~ In the past few years, several studies have compared different metrics of the tropical expansion (e.g. **???**). In contrast, the Hadley circulation ~~in~~ strength has only been compared between different reanalyses and climate models (e.g. **??**)~~, no~~. No study (to our knowledge) has yet compared the ~~measures~~ metrics of the HC strength in the same dataset. In this study, we perform such ~~an~~ inter-comparison of HC metrics and we assess how the trends estimated by different ~~measures~~ metrics compare with each other in the ERA5 and ERA-Interim reanalyses. For example, we assess ~~how sensitive are~~ the sensitivity of the trends derived from ~~measures~~ metrics based on the latitude-pressure stream-function profile (**??**) to the choice of the pressure level. Motivated by uncertainties in the results based on the different ~~measures~~metrics, we propose two alternative ~~measures~~ metrics of the HC strength: ~~a) a stream-function based measure of average strength, which also~~ 1) a stream-function-based metric of spatially-averaged HC strength, and 2) an energy metric defined as the total energy of the zonally-averaged unbalanced circulation, to which the HC is the main contributor. The first is similar to the existing metrics and grasps the overall trends of each ~~Hadley cell; and b) a normal-mode function based index which measures the strength of the global unbalanced zonal-mean circulation to which the Hadley cell makes the greatest contribution~~HC, whereas the second new metric is a more holistic approach that can be coupled to the global energy cycle but *a priori* does not distinguish between the NHC and SHC. Here

the term 'unbalanced' denotes circulation that projects on the inertia-gravity (or non-Rossby) eigensolutions of the primitive equations (e.g. **?**).

The paper is organised as follows. Section **??** describes the data and methods ~~. The measures~~ including definition of various metrics. The metrics are compared in Section **??**. Discussion and conclusions are given in Section **??**.

2 Data and Methods

2.1 Reanalysis data

Two modern ECMWF reanalyses are analysed: ERA5 (**?**) and ERA-Interim (**?**). 40 years (1979-2018) of daily data at 00 UTC are used. Meridional wind (v), zonal wind (u), specific humidity (q), and vertical velocity (ω) data are provided on 37 pressure levels between 50°S and 50°N on latitude-longitude grid with 1° resolution for both reanalyses. Among these levels, 23 are between 1000 hPa and 200 hPa.

~~The~~ A new, energy-based metric is a product of a multivariate normal-mode function ~~based index was computed using 40 years of monthly means of daily means for the zonal wind, meridional wind , temperature, geopotential and surface pressure. For details on the normal-mode function derivation and their applications, see **?** and **?**. For ERA5, the global data were analysed~~ decomposition and it requires both wind components and a pseudo-geopotential field that combines the hydrostatic geopotential and the mean sea-level pressure term (see section **??**). Input data are in this case monthly mean fields on regular Gaussian grid F80 with 1.125° horizontal resolution and 137 hybrid model levels ~~. ERA-Interim data were analysed on the same horizontal grid but using~~ for ERA5, and 60 vertical levels for ERA-Interim.

2.2 ~~Mean HC and its trend~~

~~Trends are evaluated from the time series of ψ for different point values $\psi(\varphi, p)$ as linear regression coefficients. The trends are considered significant if they pass the 95% threshold of the modified Mann-Kendall test (**?**). Note that the trends presented in this study are only representative of the analysed 40-year period and that we do not evaluate an extent to which they represent a climate-change signal. A separate study (**?**, in review) addresses this question and its results suggest that a part of the 40-year trends in the HC strength may be due to the multi-decadal variability.~~

~~Fig. **??** shows climatological monthly-mean stream function and its pointwise trends in the~~ ERA5 ~~reanalysis between 1979~~ has a higher model resolution than ERA-Interim (0.3° compared with 1°, respectively). It also has an improved dynamical core and more detailed model physics (**?**). Advanced data assimilation procedures and new observation operators allow ERA5 to assimilate five times more data than ERA-Interim. The radiative forcing depends on the long-term changes of the concentration of greenhouse gases and aerosols. The atmospheric model in ERA5 is forced by the state-of-the-art sea surface temperature (SST) and ~~2018. A significant enhancement of the winter cells can be observed: the northern Hadley cell (NHC; red contours) strengthens most between December and April, whereas the southern Hadley cell (SHC; blue contours) strengthens most between April and October. Both cells are strengthening between March and May. A prominent feature is~~

~~that the trends in the monthly-mean HC strength are spatially inhomogeneous across the cells, both meridionally and vertically. For example, from December to February, the lower-tropospheric part of the descending branch in the NHC is strengthening, while the ascending branch of the cell in the deep tropics is weakening. From July to October, the SHC exhibits significant strengthening in the ascending branch in~~ sea ice concentration (SIC) data, thus it is able to capture the low-frequency variability of the climate system better. Collectively, these upgrades result in a better agreement with the observations of tropospheric temperature, wind, humidity, and precipitation. Furthermore, the ~~Inter-Tropical Convergence Zone, while its descending branch mostly shows insignificant strengthening/weakening and even significant weakening on the southern boundary of the cell. The inhomogeneities in trends are even more pronounced in the ERA-Interim reanalysis (Fig. ??); for example, vertical inhomogeneity in the SHC trend from May to October is especially pronounced in the regions of the strongest ψ gradients. The presence of the inhomogeneities in the HC trends raises a question about the reliability of some of the climate trends derived from point measures of the HC strength.~~

~~Monthly-mean climatology of the Hadley Circulation (red and blue contours) and its trends (shading) in ERA5 reanalysis between 1979 - 2018. Red contours indicate positive climatological stream function values, i.e. $(0.1, 0.3, 0.6, 1, 1.5, 2, 2.5) \cdot 10^{11}$ kg s^{-1} and blue contours their negative equivalents, i.e. $(-0.1, -0.3, -0.6, -1, -1.5, -2, -2.5) \cdot 10^{11}$ kg s^{-1}. Crosses indicate the statistically significant trends at the 95% confidence level. Note that the overlapping of contours and shading of the same colour indicates strengthening of the cell, while overlapping of different colours indicates cell weakening.~~ accuracy of the HC estimation is boosted significantly by the reduced surface meridional wind and horizontal wind divergence bias over the oceans (**?**). Based on the above, we consider ERA5 a more reliable dataset.

2.2 ~~Measures~~ Metrics of Hadley cell strength

The trends and their uncertainties are compared for several ~~measures~~ metrics of the HC strength:

1. maximum (minimum) of annual/~~monthly-mean~~ seasonal-mean stream function between 40°S and 40°N, and between 200 hPa and 900 hPa, denoted ψ^{max} (ψ^{min}). Slightly different boundaries were employed by **???**; however, a reasonable choice of boundaries (e.g. excluding the lower part of the boundary layer and the stratosphere) does not affect the results;

2. maximum (minimum) of annual/~~monthly-mean~~ seasonal-mean stream function at predefined pressure levels (e.g. 400 hPa, 500 hPa, etc.) within 40°S and 40°N, denoted ~~ψ_p^{max} (ψ_p^{min}~~ $\psi^{max}(p)$ (or $\psi^{min}(p)$); as used in e.g. **??**~~??~~**?**;

3. stream function value at the location of climatological (1979-2018) annual/~~monthly-mean maximum /minimum~~seasonal-mean maximum (minimum) of the NHC ~~/SHC~~(SHC) strength, $\psi(\varphi^{max}, p^{max})$, where $(\varphi^{max}, p^{max}) = \underset{(\varphi,p)}{\operatorname{argmax}}(\overline{\psi_{1979-2018}})$, and analogous for $\psi(\varphi^{min}, p^{min})$;

4. an average of maximum/minimum values of annual/~~monthly-mean~~ seasonal-mean ψ over pressure levels between e.g. 200 hPa and 900 hPa, with a constant step size of 50 hPa, as in **?**:

$$\langle \psi^{max} \rangle_p = \frac{1}{N} \sum_{i=1}^{N} (\psi(p_i))^{max}, \tag{2}$$

and analogous for $\langle \psi^{min} \rangle_p$;

5. maximum of the zonal-mean velocity potential $[\Phi]^{max}(p)$ at some predefined pressure level p, typically in the upper troposphere, e.g. at 200 hPa (**?**). The velocity potential is related to the wind divergence as $\nabla \cdot \mathbf{v} = \nabla^2 \Phi$;

6. minimum of the zonal-mean vertical velocity $[\omega]^{min}(p)$, i.e. maximum ascent, at some predefined pressure level p, typically in the mid-troposphere, e.g. at 500 hPa (**?**), or a minimum ω within the tropical troposphere ($[\omega]^{min}$).

7. ~~an average~~ spatially-averaged HC strength, which is obtained by spatially averaging the stream-function field in the latitude-pressure plane. For the ~~northern HC~~NHC, it yields

$$\psi_{NHC} = \langle \psi(\varphi,p) \rangle, \quad \text{for} \quad \psi(\varphi,p) > 0 \text{ and } (\varphi,p) \in [-20°,40°] \times [50,1000] \in [-15°,45°] \times [100,1000] \text{ hPa}, \tag{3}$$

where ψ is uniformly sampled latitudinally, and vertically with a 50 hPa step. Wide latitudinal boundaries ensure that the Hadley cell is fully contained in every season (as shown in Fig. **???**). An analogous ~~measure~~ metric ψ_{SHC} is defined for the southern Hadley cell but with conditions $\psi < 0$ and meridional boundaries within ~~$\varphi \in [-40°,20°]$~~ $\varphi \in [-45°,15°]$.

8. ~~a normal-mode function based measure~~ effective wind for the water vapour transport (**?**):

$$\mathbf{v}_E = \sum_{i=1}^{N} \frac{\mathrm{PW}(i)}{\mathrm{TPW}} \mathbf{v}_D(i). \tag{4}$$

The atmospheric column is divided into N layers in Eq. **??**. In each layer i which spans from pressure level p_i to $p_{i-1} < p_i$, the amount of precipitable water is $\mathrm{PW}(i) = \frac{1}{\rho_w g} \int_{p_i}^{p_{i-1}} q(p) dp$, where ρ_w is density of liquid water. The total precipitable water in the atmospheric column is $\mathrm{TWP} = \int_{p_s}^{0} q(p) dp$. Standard notations are used: g is acceleration of gravity, q is specific humidity, $\mathbf{v}_D$ stands for divergent (irrotational) wind component, and p_s is surface pressure. The metric partially removes the influence of the change of total column water vapour (thermodynamic impact of warming climate) on the water vapour transport.

9. an energy-based metric I_M, which is defined as the total energy of the zonal-mean unbalanced circulation. ~~The index is obtained by projecting~~ Unbalanced circulation is derived using the normal-mode function decomposition and it corresponds to the circulation projecting onto the inertia-gravity eigensolutions (or IG modes) of the linearized primitive equations (**?**). The projection of global geopotential and wind fields from reanalyses onto the normal-mode functions ~~following **??**. The~~ provides time series of the complex expansion coefficients $\chi_{k,n,m}$ ~~associated with the inertia-gravity modes (IG)~~ defined by the zonal wavenumber k, vertical mode index m and meridional mode index n for each IG and Rossby eigenmode. The IG modes of the mean zonal state ($k = 0$) are ~~then~~ used to compute the total (kinetic plus available potential) energy as

$$I_M = \sum_m g D_m \sum_n \left| \chi^{\mathrm{IG}}_{k=0,n,m} \chi^{\mathrm{IG}*}_{k=0,n,m} \right|^2, \tag{5}$$

where ~~the indices m and n denote the vertical mode index and the meridional mode, respectively~~ $|\cdot|$ denotes the absolute value. For every vertical eigenmode m, D_m denotes the associated eigenvalue known as the equivalent depth (e.g. **?**, their Fig. 4), such that $D_1 > D_2 > \ldots > D_M > 0$, where M is the maximal vertical wave number. ~~To define the HC strength, only coefficients corresponding to IG modes with $k = 0$, representing the zonal-mean state, are taken into account in Eq. (??). The~~ Every combination (k, n, m) defines single component of the Hough harmonics expansion and the coupling between the geopotential height and winds. The amplitude of D_m defines the meridional scale of the modes that is associated with the radius of deformation on the equatorial $\beta-$plane, ~~a_e, which defines the trapping scale of the modes, is defined by D_m: $a_e = \sqrt{\frac{gD_m}{\beta}}$~~ $a_e = gD_m/\beta$, where $\beta = 2\Omega/R$, and Ω is Earth's angular velocity. ~~Thus, larger m-s~~ Higher modes with smaller equivalent depths correspond to stronger equatorial trapping~~,~~; e.g., for $D_7 = 708$ m the trapping scale is roughly 17°. With all vertical and meridional modes included, the mean ~~IG~~ unbalanced circulation resides mainly within the tropics, and to a small extent near the major orographic features in the extratropics and in the polar winter stratosphere, as shown in **?**, their Fig. 10~~using ERA-Interim. For more~~. For details on the ~~modal decomposition, see Appendix A~~derivation and application of normal-mode functions the reader is referred to **?**. Two figures in Appendix illustrate the new metric. First, Fig. **??** shows the unbalanced circulation at 200 hPa level for four seasons illustrating that its seasonal march across the equator resembles the Hadley cell. Figure **??** ~~shows~~ confirms that the Hadley circulation is well represented by ~~the zonal-mean unbalanced (IG) circulation (compare Fig. **??**b vs. Fig. **??**a).~~ our new metric.

The described ~~indices~~ metrics have different properties. ~~Indices~~ Metrics (1)-(4)~~and~~ , (7) and (8) distinguish between the two Hadley cells, whereas ~~indices~~ metrics (5), (6) and (~~8~~9) do not. ~~Indices~~ Metrics (1) to (3) ~~do not capture~~ are sensitive to the vertical inhomogeneities in the strength of the Hadley cell by definition. ~~Index~~ Metric (8) describes only the return flow of the Hadley circulation in the lower troposphere. Metric (4) ~~captures~~ averages over the vertical but not the meridional inhomogeneity. ~~Indices~~ Metrics (5) and (6) only describe the ascending branch of the Hadley circulation. New ~~measure~~ metric (7) ~~by definition does not describe spatial inhomogeneities, but captures them~~ alleviates the sensitivity to the spatial (meridional and vertical) inhomogeneties by spatial averaging. The same applies to the new ~~measure (8~~metric (9), which is ~~by definition a global measure, but in large part explained by the Hadley circulation (Fig. **??**) and also does not distinguish between the two HCs.~~ a global metric largely different from all other metrics, and applied here without any special tuning. Metrics (8) and (9) include nonlinear terms (Eqs. (**??**)-(**??**)), therefore the metrics are sensitive to the temporal averaging of the input data (e.g. hourly means, daily means, monthly means of daily means). In this study, monthly means are used for metric (8), consistent with **?**, whereas metric (9) uses monthly means due to computational complexity.

In the following section, we explore the sensitivity of the trends to different ~~measures~~ metrics of the HC strength.

3 Sensitivity of the Hadley circulation trends to different ~~measures~~metrics

3.1 ~~Comparison of the stream-function based measures~~Mean HC and its trend

Trends are evaluated from the time series of ψ for different single-point values $\psi(\varphi,p)$ as linear regression coefficients. The trends are considered significant if they pass the 95% threshold of the modified Mann-Kendall test using the trend-free pre-whitening method to eliminate the impact of serial autocorrelation (**??**). Note that the trends presented in this study are only representative of the analysed 40-year period and that we do not evaluate the extent to which they represent a climate-change signal. A separate study (**?**, in review) addresses this question and its results suggest that a part of the recent 40-year trend in the HC strength may be due to the multi-decadal variability.

Fig. **??** shows climatological seasonal-mean stream function and its pointwise trends in the ERA5 reanalysis between 1979 and 2018. A significant enhancement of the winter cells can be observed: the northern Hadley cell (NHC; red contours) strengthens most in December-January-February (DJF), whereas the southern Hadley cell (SHC; blue contours) strengthens most in June-July-August (JJA). Both cells are strengthening between March and May (MAM). Note that trends in the seasonal-mean HC strength are spatially inhomogeneous across the cells, both meridionally and vertically. For example, in the winter NHC (DJF), the lower-tropospheric part of the descending branch is mostly strengthening, while the ascending branch of the cell in the deep tropics is weakening. From September to November (SON), the SHC exhibits significant strengthening in the ascending branch in the Inter-Tropical Convergence Zone, while its descending branch mostly shows insignificant strengthening/weakening and even significant weakening at the southern boundary of the cell. The inhomogeneities in trends are even more pronounced in the ERA-Interim reanalysis (Fig. **??**); for example, vertical inhomogeneity in the SHC trend in MAM, JJA and SON is especially pronounced in the regions of the strongest ψ gradients. The presence of the inhomogeneities in the HC trends raises a question about the reliability of some of the trends derived from single-point metrics of the HC strength.

3.2 Comparison of the stream-function metrics

The sensitivity of the trends of the annual-mean and ~~monthly-mean~~ seasonal-mean HC strength to the ~~stream function-based measures~~ stream-function metrics (1)-(4) and (7), described in Section 2.3, is shown in Fig. **??** for ERA5 and in Fig. **??** for ERA-Interim. In both reanalyses, large differences are observed between the trends of $\psi^{max}(p)$ at distinct pressure levels p (~~measure~~ metric (2)). In ERA5, the multiyear trend of the annual-mean NHC (leftmost column in Fig. **??**a) is $0.7{\cdot}10^8$ kg s^{-1} yr^{-1} at 400 hPa and ~~2.3~~2.2$\cdot 10^8$ kg s^{-1} yr^{-1} at ~~750~~ 800 hPa. For the SHC (Fig. **??**b), $\psi^{min}(p)$ strengthens by $0.9{\cdot}10^8$ kg s^{-1} yr^{-1} at 800 hPa and by $2.8{\cdot}10^8$ kg s^{-1} yr^{-1} at 400 hPa. In ERA-Interim, the NHC exhibits even differences in the sign of trends (leftmost major column in Fig. **??**a); a strengthening trend of ~~$2 \cdot 10^8$~~ $1.9 \cdot 10^8$ kg s^{-1} yr^{-1} is present at ~~750 hPa and a~~ 700 hPa and an insignificant weakening trend of ~~$-0.4 \cdot 10^8$~~ $-0.3 \cdot 10^8$ kg s^{-1} yr^{-1} at ~~450~~ 400 hPa. The SHC has an insignificant trend of the annual-mean HC in the lower troposphere and a significant weakening of up to $-3 \cdot 10^8$ kg s^{-1} yr^{-1} in the upper troposphere (leftmost major column in Fig. **??**b), i.e. opposite to what ERA5 shows.

The differences between trends of ~~monthly-means~~ seasonal-means at different pressure levels are even larger. For example, the ~~February~~ winter NHC exhibits a large and significant strengthening in the lower troposphere (~~700 hPa - 800~~ 700-800 hPa) with trends around ~~$7 \cdot 10^8$~~ $4.5 \cdot 10^8$ kg s^{-1} yr^{-1} in both ERA5 (Fig. **??**a) and ERA-Interim (Fig. **??**a); however the trends in the mid-troposphere (~~400 hPa - 500~~ 400-500 hPa) are ~~negative and mostly~~ mostly negative and/or insignificant. Different

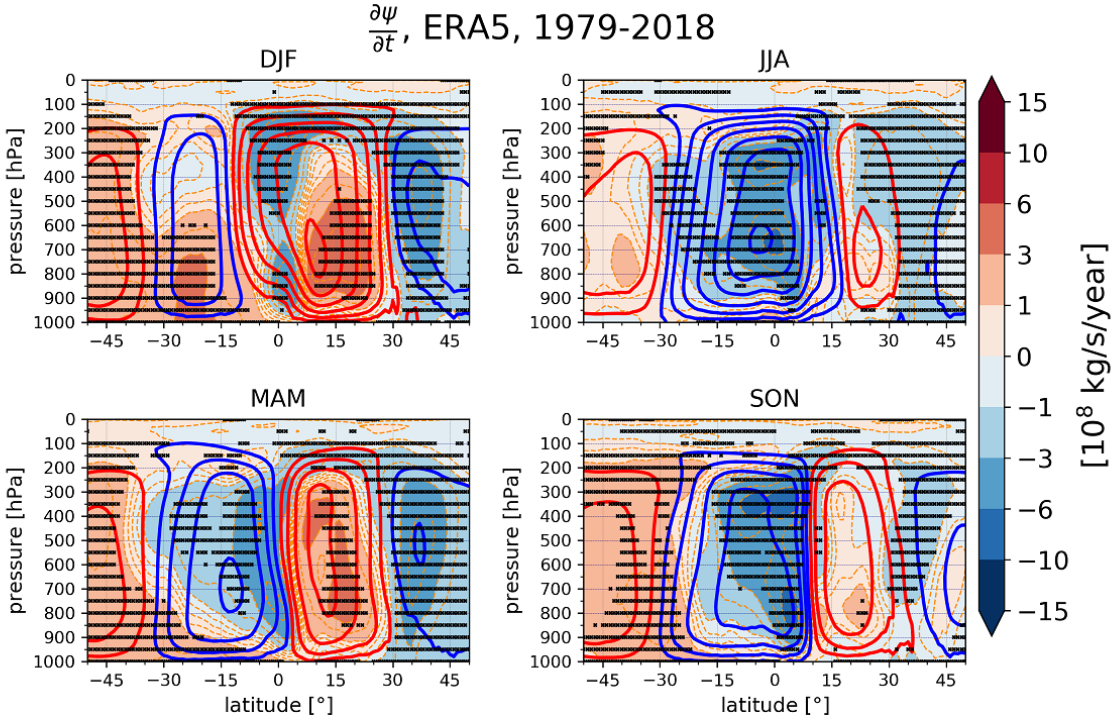

Figure 1. Seasonal-mean climatology of the Hadley Circulation (red and blue contours) and its trends (shading) in ERA5 reanalysis between 1979 - 2018. Red contours indicate positive climatological stream-function values, i.e. $(0.1, 0.3, 0.6, 1, 1.5, 2, 2.5) \cdot 10^{11}$ kg s^{-1} and blue contours their negative equivalents, i.e. $(-0.1, -0.3, -0.6, -1, -1.5, -2, -2.5) \cdot 10^{11}$ kg s^{-1}. Crosses indicate the statistically significant trends at the 95% confidence level. Note that the overlapping of contours and shading of the same colour indicates strengthening of the cell, while overlapping of different colours indicates cell weakening.

magnitudes of the trends at distinct pressure levels can partly be explained by the differences in the climatological-mean magnitude of the HC strength at different pressure levels. ~~In general, the greater the mean HC magnitude, the greater the trend. The same feature can be observed in Fig. ??~~Normalization accounts for some of these differences; normalized results are discussed below at the end of Section 3.2 (see Figure **??**).

The differences in the trends of ~~monthly-means~~ seasonal-means at various pressure levels point ~~at~~ towards the unreliability of the trend. Furthermore, magnitudes of the differences between ~~indices~~ metrics are of the same order as the uncertainties of the derived trends for individual ~~indices~~metrics. Thus, by measuring the maximum HC strength at a selected pressure level, e.g. 500 hPa (as in ~~measure~~ metric (2)), the estimated trends are affected by the limitation of the ~~measure. At this level, the HC strength also exhibits a greater year-to-year variability of annual-mean and particularly monthly-mean variability (not shown), and consequently an increased uncertainty in the trend~~metric.

Another notable feature of Figs. **??**b and **??**b is a significant difference between the trends of the annual-mean SHC strength in ERA5 and ERA-Interim reanalyses; the SHC is strengthening in ERA5 but weakening in ERA-Interim. ~~From July to October~~

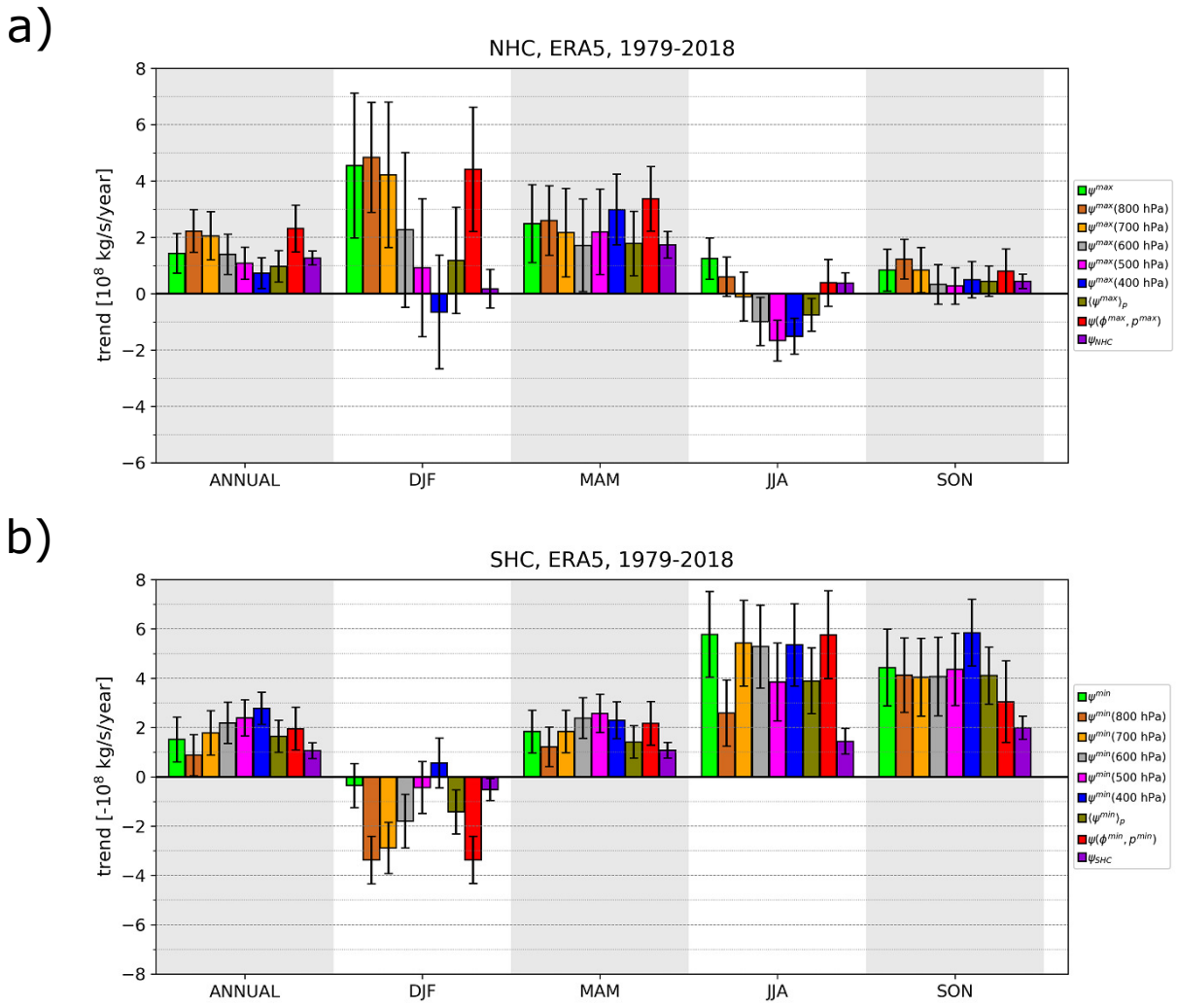

Figure 2. Trends of the NHC strength (a) and SHC strength (b) in ERA5 reanalysis between 1979-2018 for different ~~stream-function-based measures~~ stream-function metrics from Section ~~??~~??. Annual-mean trends of the HC strength are shown in the first column, while ~~monthly-mean~~ seasonal-mean trends are shown in the other columns (as labeled). Different ~~measures~~ metrics of the HC strength are shown in the legend, e.g. in (a) for the NHC: ψ^{max} denotes annual/~~monthly stream function~~ seasonal stream-function maximum (~~measure~~ metric (1)), ψ^{max} at 400 hPa, ~~450~~ 500 hPa, etc. denotes annual/~~monthly stream function~~ seasonal stream-function maximum at respective pressure level (~~measure~~ metric (2)), and $\psi(\varphi^{max}, p^{max})$ denotes that the trends are measured at the point of the maximum stream function in a multiyear average of the NHC strength (~~measure~~ metric (3)). $\langle\psi^{max}\rangle_p$ denotes vertically averaged ψ^{max} between 200 hPa and 900 hPa (~~measure~~ metric (4), Eq. **??**) and ψ_{NHC} denotes ~~measure~~ metric of ~~average~~ spatially-averaged HC strength (~~measure~~ metric (7), Eq. ~~??~~??). Analogous notations are used for the ~~stream function~~ stream-function minimum for the SHC in (b). Note that values in (b) are multiplied by (-1), thus positive values in both (a) and (b) indicate strengthening of the cell. Black error bars indicate standard error of the trend estimates.

In JJA and SON, the SHC is strengthening in both reanalyses ~~, while from April to June it~~ by the majority of metrics, while in MAM, SHC is weakening in ERA-Interim and strengthening in ERA5. The reasons for such discrepancies are likely in the data assimilation modelling and treatment of observations, and are therefore beyond the scope of this study.

~~Measure~~ Metric (1) exhibits significant year-to-year variability in the levels of ψ^{max}, observed also by **?**. ψ^{max} is switching between 350 hPa and 700 hPa levels in ERA5, and between 400 hPa and 650 hPa levels in ERA-Interim (Fig. **??**, magenta and red lines). In contrast, the level of ψ^{min} remains roughly the same (700-750 hPa, blue and orange lines in Fig. **??**) in both reanalyses throughout the studied period. ~~Measure~~ Metric (1) also sometimes produces anomalous trends especially in the seasonal data, which do not align with any of the other ~~measures~~ metrics (e.g. in ~~June and July NHC in ERA5, Fig. **??**a~~ERA5 NHC in JJA).

~~Measure~~ Metric (2) ~~does not capture~~ is sensitive to the vertical inhomogeneity in the trend of the HC strength (as seen from ψ at different levels in Figs. **??**, **??**). ~~Measure~~ Metric (3) evaluates each Hadley cell in a spatially-fixed point throughout the observed period (1979-2018 in our study). Thus, we expect it to be susceptible to potential meridional shifts of the mean Hadley circulation (**?**) or vertical shifts due to vertically expanding tropical troposphere (**?**). As a single-point ~~measure~~metric, it also suffers from spatial inhomogeneity of the trend of the HC strength, similar to ~~measure (2). It can also produce spurious trends, such as the SHC trends in November in ERA5 (Fig. **??**b, red bar) , where the climatological maximum of the SHC is located at the Equator at 850 hPa pressure level (Fig. **??**).~~ metrics (1) and (2).

Vertically averaged maximum/minimum values of ψ as in ~~measure~~ metric (4) reduce the discrepancies associated with the varying pressure levels of stream-function maxima and minima. ~~Measure~~ Metric (4) also grasps the differences in the trends of the HC strength and averages them. Furthermore, such a ~~measure~~ metric averages out the differences between the trends at different pressure levels, as well as the uncertainty due to the choice of the pressure level in ~~measure~~ metric (2). However, Fig. ~~**??**~~ **??** also revealed significant trend inhomogeneities in the meridional direction, e.g. between the ascending and the descending branches of the Hadley circulation, which are addressed by the ~~measure of average~~ metric of spatially-averaged HC strength (i.e., by adding a meridional average).

The HC strength measured by (7) is on average weaker than in other ψ-based ~~measures~~ metrics as spatial averaging leads to smaller magnitude of ψ (not shown). Consequently, ~~also~~ the trends are smaller (Figs. **??**, **??**, rightmost violet bar in each major column). When trends are spatially more homogeneous, ~~measure~~ metric (7) exhibits relatively smaller uncertainties than the other ~~measures~~ metrics (e.g. trends in ~~monthly~~ seasonal means of the NHC ~~from March to May~~in MAM, ERA5, Fig. ~~**??**~~ **??** and Fig. **??**a), and conversely for spatially less homogeneous trends (e.g. trends in ~~monthly-means~~ seasonal-means of the NHC ~~from July to September and December~~in JJA, ERA5, Fig. ~~**??**~~ **??** and Fig. **??**a). The ~~average HC measure~~ spatially-averaged HC metric (7) thus provides an average over "extreme" local HC strength ~~measures~~ metrics (1-4), as well as an overall uncertainty. ~~Note that~~ Figs. **??**, **??** ~~merely showcase~~ reflect the stronger year-to-year variability of ~~monthly~~ seasonal means (compared with year-to-year variability of annual means), as well as ~~large~~ larger discrepancies between ψ~~-measures~~ -metrics at different levels (as also seen from Figs. ~~**??**, **??**), however~~ **??**, **??**). However from here on, we limit the analysis only to the trends ~~of the annual-mean~~ (and variability) of the *annual-mean* Hadley circulation.

3.3 Comparison of ~~stream-function-based measures~~ stream-function metrics with other ~~measures~~metrics

The time-series ~~of measures~~ $X(t)$ of metrics with different units and different mean magnitudes can be compared after their normalisation ~~which is in our case~~ by their respective climatological value ~~for~~ of the 1979-2018 period ~~, denoted $\langle\psi\rangle$.~~ (denoted $\overline{X}$). Results are shown in Fig. **??** for ERA5 reanalysis, including the normalized time-series of ~~stream-function-based~~ stream-function (ψ) ~~measures~~ metrics (1)-(4) and (7), velocity-potential (Φ) ~~based measures~~ metrics (5), pressure-velocity (ω) ~~based measures~~ metrics (6), ~~and measure (8~~water vapour transport metric, and metric (9) describing the total energy of the zonal-mean unbalanced circulation. Figure **??** and Table **??** present the trends of the normalized time-series, i.e. the relative trends ~~$(\partial\psi/\partial t)/\langle\psi\rangle$~~ $(\partial X/\partial t)/\overline{X}$ in percentages per year, whereas Fig. **??** shows the correlations between the time-series of HC strength derived from different ~~measures~~metrics.

In general, the normalized ~~indices~~ metrics are well aligned in both HCs (Fig. **??**, in grey colours), with a slightly larger spread over a few periods (e.g. 1979-1982 in both HCs). The time-series of ψ~~-indices~~-metrics are better aligned for the SHC than the NHC, both in ERA5 and ERA-Interim (Fig. **??**). They are also highly correlated (Fig. **??**), as expected from Fig. **??**. For example, the time-series derived from $\psi^{max}(p)$ (~~measure~~ metric (2)) at ~~neighbouring~~ nearby pressure levels (~~50~~ 100 hPa apart) are highly correlated with correlation coefficient ~~$r > 0.98$, whereas~~ $r > 0.94$~~for measures 100 hPa apart~~. Absolute ψ^{max} ~~(measure~~ and ψ^{min} (metric (1)) ~~correlates~~ correlate best with $\psi^{max}(p)$ ~~at mid-tropospheric presssure levels (550-650 hPa), whereas absolute ψ^{min} correlates best with~~ and $\psi^{min}(p)$ at ~~lower-tropospheric presssure levels (650-800~~ lower-to-mid-tropospheric pressure levels (500-800 hPa). The result is in line with Fig. **??**. Normalized ~~measure~~ metric (4) is highly correlated ($r > 0.9$) with $\psi^{max}(p)$ and $\psi^{min}(p)$ at various levels.

A widely utilized HC strength ~~measure~~ metric $\psi^{max}(500\,\mathrm{hPa})$ (and similarly ψ^{max}) also highly correlates (~~$r = 0.88$~~$r = 0.85$) with the ~~average HC strength measure~~ spatially-averaged HC strength metric (7), ψ_{NHC}. ~~However, in~~ In the SHC, the ~~stream function~~ stream-function minimum at 500 hPa ~~only moderately correlates ($r = 0.77$~~yields a slightly lower correlation ($r = 0.81$) with the ~~average SHC strength~~ spatially-averaged SHC strength metric, ψ_{SHC}. ~~On the other hand, ψ^{min}~~ Even higher correlations ($r = 0.87$) with the spatially-averaged SHC strength are found for $\psi^{min}(p)$ at 700 hPa and ~~750 hPa has a high correlation with the average HC strength ($r = 0.86$). These~~ ψ^{min}.

The above results suggest that the ~~ψ^{max}-measures~~ $\psi^{max}(p)$ metrics at pressure levels between 600 hPa and 500 hPa are most representative of the overall changes in the NHC, whereas ~~ψ^{min} measures between 750 hPa and~~ $\psi^{min}(p)$ metrics around 700 hPa are most representative ~~for~~ of the SHC. The other single levels should probably be avoided as the ~~HC strength indices~~metrics of the overall HC strength.

~~Time-series~~ The time-series of the other ~~measures~~stream-function metrics, i.e. ψ^{max} or ψ^{min}, $\langle\psi^{max}\rangle_p$ or $\langle\psi^{min}\rangle_p$, $\psi(\varphi^{max}, p^{max})$ or $\psi(\varphi^{min}, p^{min})$ at the location of the climatological maximum or minimum ~~all~~ also highly correlate (~~$r = 0.82$ to 0.88~~$r = 0.80$ to 0.89) with the ~~average HC strength measure as well~~spatially-averaged HC strength metric (7). This means that the newly proposed ~~average measure~~ metric (7) is an adequate candidate for assessing the changes of the HC strength.

Despite the high correlations, the relative trends of ψ~~-indices~~-metrics can differ significantly (Fig. **??**~~), especially in ERA-Interim~~; Tables **??**, **??**). ERA5 (Fig. **??**a,c; Table **??**) shows mostly significant strengthening from 0.09-0.36% yr^{-1}

for the NHC and 0.08-0.32% yr^{-1} for SHC~~(Table ??)~~. In the NHC, the widely used ~~measure~~ metric ψ^{max} (500 hPa) shows strengthening of 0.14% yr^{-1} and is equal to the trend of $\langle\psi^{max}\rangle_p$, while ψ^{max} increases by 0.18% yr^{-1}. $\psi(\varphi^{max}, p^{max})$ and ψ_{NHC} show larger trends with strengthening of 0.29% yr^{-1} and 0.36% yr^{-1}, respectively. The two ~~measures which~~ metrics that perform spatial averaging, ~~$\langle\psi^{max}\rangle_p - \langle\psi^{min}\rangle_p$~~ and ψ_{SHC}, suggest strengthening of the southern cell by 0.18% yr^{-1} and ~~0.22~~0.23% yr^{-1}, respectively. The relative trends derived from the ~~average HC strength measure~~ spatially-averaged HC strength metric (7) show ~~mildly~~ reduced uncertainty compared to the other stream-function-based ~~point measures~~single-point metrics, in line with the results of Section **??**.

The time-series derived from ω~~-indices~~-metrics have much higher temporal oscillations compared with ψ~~-indices~~-metrics (Fig. **??**), however the maxima and minima are fairly aligned with ψ~~-indices~~-metrics, though with larger anomalies~~, which~~. This is captured also by their moderate correlations ($r = 0.3$ to 0.5 for the SHC and 0.4 to 0.65 for the NHC) (Fig. **??**, **??**). However, the ~~average~~ spatially-averaged HC strength (~~measure~~ metric (7)), ψ_{NHC} and ψ_{SHC}, correlates better with the ω~~-indices~~-metrics: $r =$ ~~0.67 to 0.80~~ 0.70 to 0.81 for the NHC and ~~0.63 to 0.71~~ 0.65 to 0.72 for the SHC. The ~~measure~~ metric (7) also correlates better with the Φ~~-indices than~~-metrics than the other ψ~~-indices~~-metrics, particularly with $[\Phi]^{max}$ at 200 hPa and 250 hPa. This further implies that the ~~average~~ spatially-averaged HC strength (~~measure~~ metric (7)) captures also the changes in the HC in regions of ascending motion. The correlation of $[\Phi]^{max}$ at 150 hPa with other ~~measures~~ metrics is low and mostly insignificant, suggesting that the 150 hPa level might already be in the tropical tropopause.

The ~~velocity-potential-based measures~~ velocity-potential metrics $[\Phi]^{max}(p)$ show much larger magnitude of the trends compared with the other ~~measures~~metrics. They are also very susceptible to the applied pressure level, a similar issue as for the ψ~~-indices~~-metrics. Therefore, this ~~measure~~ metric is also likely susceptible to the potential future changes in the depth of the tropical troposphere. For example, $[\Phi]^{max}$ (250 hPa) in ERA5 shows a strengthening trend of 1.14% yr^{-1}, at 200 hPa roughly 0.11% yr^{-1}, whereas $[\Phi]^{max}$ at 150 hPa shows a weakening trend of -0.38% yr^{-1} (Fig. **??**a; Table **??**), an outlier among the other ~~measures~~metrics. The differences among trend magnitudes are even larger in ERA-Interim (Fig. **??**b; Table **??**).

The trends derived from the ω~~-indices~~-metrics align reasonably well with the trends derived from the ψ~~-indices~~-metrics. In particular, $[\omega]^{min}$ at 500 hPa (dark grey bar in Fig. **??**) shows good agreement with the ~~average~~ spatially-averaged HC strength (~~measure~~ metric (7)), but with more than ~~twice as large~~ doubled uncertainty due to larger variability of the ω~~-indices~~-metrics, as revealed in Fig. **??**. As for the other ~~point measures~~single-point metrics, the derived trends of the ω-based HC strength are strongly susceptible to the choice of ~~a~~ the pressure level (this is again more pronounced in the ERA-Interim).

The effective wind metric (8) aligns well with the stream-function metrics (Fig. **??**), as reflected in their high correlations ($r = 0.68 - 0.86$) for the NHC and moderate correlations ($r = 0.43 - 0.52$) for the SHC. The exception is the high correlation ($r = 0.8$) of metric (8) with spatially-averaged metric ψ_{SHC}. The sign and the magnitude of the HC strength defined by metric (8) also aligns well with the stream-function-based metrics, except for SHC in ERA-Interim. On the other hand, for the NHC, the effective wind metric (8) shows low (and insignificant) correlations with ω- and Φ-metrics describing the ascending branch of the HC, whereas it shows high correlations ($r \sim 0.7$) for the SHC (in both reanalyses). These results likely suggest that the northward water vapour transport to the deep tropics provides the bulk of the fuel for condensation, associated vertical motions and divergent outflow in the upper troposphere (described by the velocity potential).

Table 1. Annual-mean HC strength trends normalized by the climatological-mean values of the HC strength in ERA5 between 1979-2018. The trends derived from stream-function ~~based measures~~ metrics (which distinguish between the NHC and the SHC), are separated by the horizontal black line from the trends, derived from other ~~measures~~ metrics (which describe the two cells together). The values in the parentheses denote standard error of the trend estimates.

NHC ~~measure~~ metric	trend (± unc.) [%/yr]	SHC ~~measure~~ metric	trend (± unc.) [%/yr]	HC ~~measure~~ metric	trend (± unc.) [%/yr]
ψ^{max}	0.177 (± 0.087)	ψ^{min}	0.136 (± 0.081)	$[\Phi]^{max}$ (150 hPa)	-0.375 (± 0.121)
ψ^{max} (800 hPa)	0.304 (± 0.104)	ψ^{min} (800 hPa)	0.082 (± 0.079)	$[\Phi]^{max}$ (200 hPa)	0.110 (± 0.126)
ψ^{max} (750 hPa)	0.298 (± 0.108)	ψ^{min} (750 hPa)	0.125 (± 0.080)	$[\Phi]^{max}$ (250 hPa)	1.136 (± 0.140)
ψ^{max} (700 hPa)	0.258 (± 0.108)	ψ^{min} (700 hPa)	0.160 (± 0.081)	$[\omega]^{min}$ (400 hPa)	0.519 (± 0.170)
ψ^{max} (650 hPa)	0.213 (± 0.102)	ψ^{min} (650 hPa)	0.192 (± 0.082)	$[\omega]^{min}$ (500 hPa)	0.349 (± 0.178)
ψ^{max} (600 hPa)	0.178 (± 0.091)	ψ^{min} (600 hPa)	0.214 (± 0.082)	$[\omega]^{min}$ (600 hPa)	0.412 (± 0.187)
ψ^{max} (550 hPa)	0.157 (± 0.080)	ψ^{min} (550 hPa)	0.233 (± 0.081)	$[\omega]^{min}$	0.738 (± 0.155)
ψ^{max} (500 hPa)	0.140 (± 0.073)	ψ^{min} (500 hPa)	0.257 (± 0.079)	I_M	0.072 (± 0.074)
ψ^{max} (450 hPa)	0.116 (± 0.070)	ψ^{min} (450 hPa)	0.280 (± 0.077)		
ψ^{max} (400 hPa)	0.094 (± 0.070)	ψ^{min} (400 hPa)	0.319 (± 0.075)		
$\psi(\varphi^{max}, p^{max})$	0.294 (± 0.106)	$\psi(\varphi^{min}, p^{min})$	0.177 (± 0.079)		
$\langle\psi^{max}\rangle_p$	0.136 (± 0.077)	$\langle\psi^{min}\rangle_p$	0.183 (± 0.073)		
~~ψ^{NHC}~~ ψ_{NHC}	0.358 (± 0.071)	ψ_{SHC}	~~0.223~~ 0.232 (± 0.070)		
v_E^{NHC} (1000-850 hPa)	0.103 (± 0.078)	v_E^{SHC} (1000-850 hPa)	0.333 (± 0.076)		

The total energy of the zonal-mean unbalanced circulation I_M has strengthened in the 1979-2018 period in both ~~ERA5 and ERA-Interim~~ reanalyses with a rate of ~~0.07% yr^{-1} and 0.28~~roughly 0.1% yr^{-1} (Fig. **??**; Tables **??**, **??**). The uncertainty of the trend is ~~relatively small compared to the other measures (Tables **??**, **??**). The~~ smaller than in the other metrics. For ERA5, the sign of the derived trends ~~in ERA5~~ is consistent with ~~other measures in ERA5, although the magnitude is smaller~~the other metrics. However, the I_M metric suggests strengthening of the ~~global unbalanced circulation~~ HC also in ERA-Interim (Fig. **??**b,d)~~, a trend opposite to that~~. This global trend in the HC strength is consistent with strengthening of the NHC derived from the ~~stream-function-based indices~~other metrics in ERA-Interim, but is opposite to their trends of the SHC. Furthermore, the correlation of the ~~unbalanced energy index with other indices~~ energy metric with the other metrics is low and insignificant (Fig. **??**), except for the $[\Phi]^{max}$ at 150 hPa. Insignificant correlations are not surprising as this ~~index~~ metric is largely different from all other ~~indices~~metrics. First, it is the total energy ~~measure~~metric; the kinetic energy ~~part~~ is due to both components of the horizontal flow and there is a contribution to the energy ~~comes also from outside the tropics~~ also from extratropical troposphere and from the stratosphere. ~~We argue that the~~ The part of I_M from the extra-tropics and the stratosphere is however arguably unimportant for the overall ~~signal, but it may be important for the trends. **?** discussed~~ magnitude of the metric. **?** discussed the unbalanced circulation in ERA5 and ERA-Interim in relation to ~~the data assimilation behind the two reanalyses. They~~ their

observation processing and data assimilation setups, and showed that in spite of the differences, the two datasets agree on the ~~positive trend~~ trends in the most energetic large-scale features of tropical circulation.

To quantify the role of the stratospheric circulation ~~to the uncertainties in the trends in~~ in the uncertainties of the trends for the I_M metric, we compared I_M in ERA-Interim focusing on levels up to ~~100 hPaonly~~about 93 hPa. It revealed a smaller~~trend though still positive~~, but still positive trend in ERA-Interim and a somewhat higher correlation with the other ~~indices~~ metrics (not shown).

Given the importance of the mixed Rossby-gravity (MRG) waves in the Hadley circulation ~~(?)~~(??), we also tested an extension of the I_M, ~~which consists of adding the MRG wave energy to the zonal-mean unbalanced energy~~ that includes also energy of the MRG waves for all zonal wavenumbers in Eq. (??). In this case, the relative trend increased by a ~~slight~~ small margin, while the correlation with ~~other measures~~ the other metrics remained insignificant (not shown). Furthermore, performing the summation (Eq. ??) for a subset of vertical modes (e.g. $m \geq 9$), thereby reducing the stratospheric and high-latitude contributions to the I_M, ~~results both in greater correlations with other measures, and in a larger relative trend, which is better aligned with other measures~~ improved correlations with the other metrics, and also increased a trend, in a better alignment with the other metrics (not shown).

4 Conclusions and Outlook

In this study, we have analysed a number of ~~indices~~ metrics of the Hadley circulation strength including ~~indices~~ metrics based on the mass-weighted mean meridional stream-function, velocity potential, pressure velocity ω, water vapour transport, and the total energy of the zonal-mean unbalanced circulation. The ~~indices~~ metrics were applied to ERA5 and ERA-Interim reanalysis data between 1979 and 2018. While ERA5, a more recent and a more reliable reanalysis, is our main dataset, its comparison with ERA-Interim provides confidence that the observed ~~characteristics of a particular measure~~ discrepancies between distinct metrics are not an isolated feature of ERA5 reanalysis. However, the comparison is not ~~straightfoward~~ straightforward as the two reanalyses differ in their ~~representation of the unbalanced tropical circulation. This was made evident by a new HC strength measure defined as the global total energy of the unbalanced zonal-mean circulation. Another newly proposed measure~~ representations of the tropical circulation, including uncertainties that are difficult to quantify. These involve uncertainties in observations, differences in data assimilation methodology, and general model differences. We have also proposed two new metrics that are based on averaging or integrating circulation properties to alleviate the character of some existing metrics. The first newly proposed metric describes the average strength of the NHC and SHC using ~~the average~~ spatially-averaged stream function and is therefore insensitive to spatial inhomogeneities. The other new metric quantifies the total energy of the unbalanced zonal-mean circulation.

By analysing the ~~temporal changes of the stream function changes~~ stream-function trends in the latitude-pressure plane, we showed that the ~~HC strength~~ trends are spatially inhomogeneous, both meridionally and vertically (Figs. ~~??~~,~~??~~??,??), particularly in ERA-Interim. ~~Distinct HC strength measures~~ Therefore, distinct stream function metrics of the HC strength resulted in significantly different and sometimes even opposing trends, decreasing our prospects to draw firm conclusions on

the circulation changes. The ~~two new measures~~ same applies to other single-point metrics of the HC strength. The two new metrics of the HC strength are characterized by a smaller uncertainty of the derived trends compared to the current ~~measures of the HC strength~~metrics, likely due to spatial averaging (average stream function) or the integration (total energy of zonal-mean unbalanced circulation). ~~However, the normal modes based index is affected by its global definition meaning that the unbalanced zonal-mean circulation outside the tropical and subtropical troposphere is also accounted for. Future work can refine the index.~~

~~In light of all the results, we recommend using the measure of the average HC strength (measure (7) in Section ??) whenever interested in the variability and trends of the HC strength. Having said this, usage of new and established measures will ultimately depend on the purpose of a study.~~

Presented opposing trends suggest that the contribution of physical mechanisms that drive the Hadley cells and govern their strength (~~e.g.~~ diabatic heating, friction, eddy heat and momentum fluxes, static stability, etc.) are likely to vary with the chosen HC strength ~~measure (??)~~metric (**??**, in review). For example, ~~the~~ friction should affect the HC strength trends more if the ~~measure~~ metric $\psi^{max}(p)$ is taken at some lower-tropospheric pressure level, whereas its impact is likely reduced when $\psi^{max}(p)$ is evaluated at mid-to-upper tropospheric levels. ~~However,~~ Note that a detailed analysis of these effects is beyond the scope of this study and will be pursued in the future.

~~Our results confirm~~ Because of the different mechanisms involved in the HC dynamics, the choice of the HC strength metric will ultimately depend on the application in a specific study. However, our results demonstrate that caution is needed when comparing HC trends from different studies using different ~~measures~~ metrics of the HC strength. ~~A unified index of the Hadley circulation would~~ In light of all the results, we therefore recommend using the spatially-averaged stream function as the metric of the HC strength (metric (7) from Section **??**) whenever interested in the variability and trends of the overall HC strength. We also suggest an introduction of a unified metric of the HC strength (e.g. metric (7)) that will allow an easier comparison of the different studies on the topic of the *overall* HC strengthening/weakening. This would also allow a better estimation of the likelihood of the future changes in the global atmospheric circulation ~~(e.g., ?)~~(e.g., **?**).

Code and data availability. Scripts are available upon request. The ERA-Interim and ERA5 reanalysis datasets are available from http://www.ecmwf.int. The data were obtained using Copernicus Climate Change Service information 2021. Data used to generate Figs. 2 to 5 and Figs. A3 to A6 are publicly available at https://github.com/zaplotnik/Hadley-cell-strength and published in Zenodo data repository: https://zenodo.org/record/5135222#.YPzCMXUzb6c.

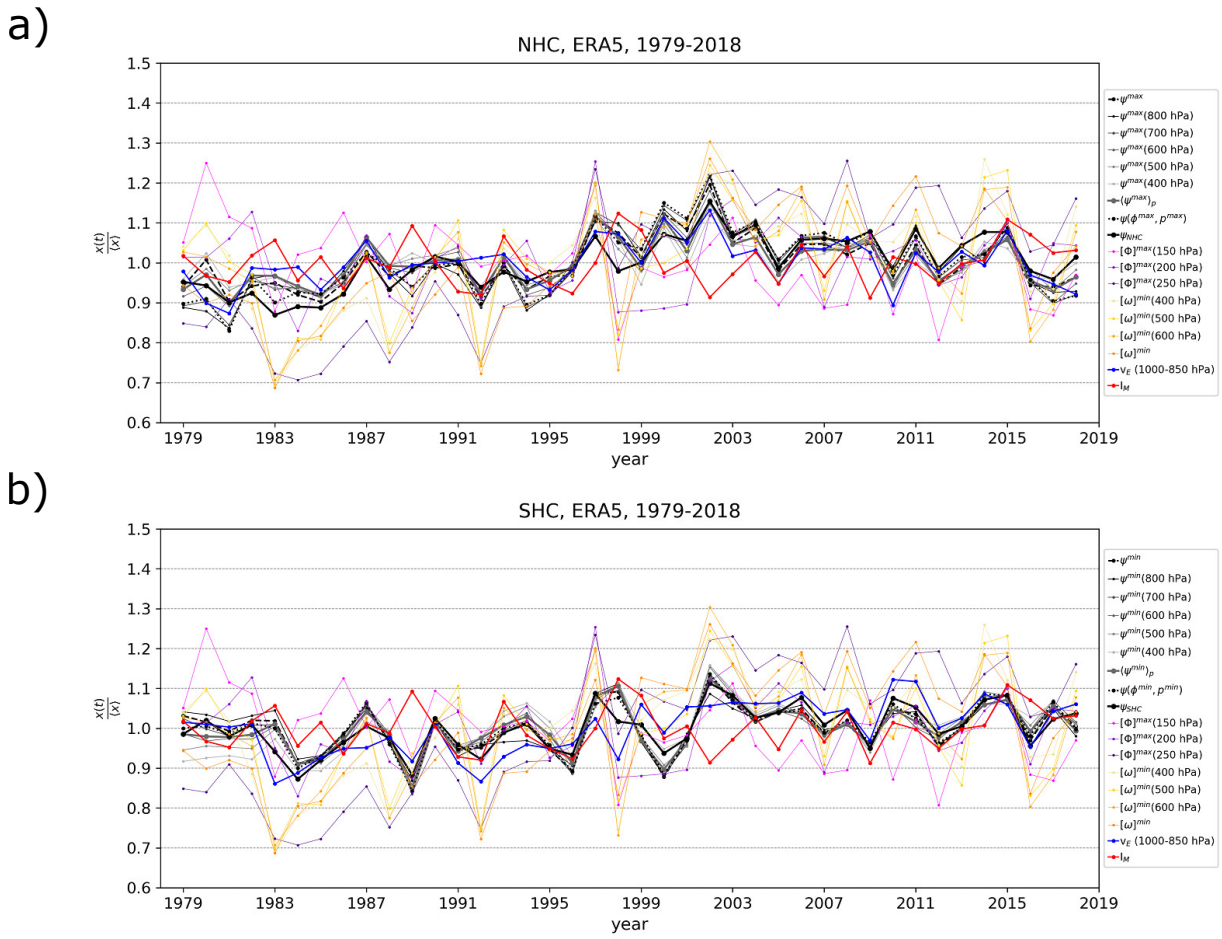

Figure 3. Time-series of the NHC strength (a) and the SHC strength (b) in ERA5 reanalysis between 1979-2018 for different ~~measures~~ metrics from Section ~~??~~??. Time-series are normalized by their 1979-2018 climatological mean. Different ~~stream-function-based measures~~ stream-function metrics of the HC strength are shown in the legend (in grey colours), e.g. in (a) for the NHC: ψ^{max} denotes the annual/~~monthly stream function~~ seasonal stream-function maximum (~~measure~~ metric (1)); ψ^{max} at 800 hPa, ~~750~~ 700 hPa, ~~700~~ 600 hPa, etc. denotes the annual/~~monthly stream function~~ seasonal stream-function maximum at respective pressure level (~~measure~~ metric (2)); $\psi(\varphi^{max}, p^{max})$ denotes that the HC strength is measured at the point of the maximum stream function in a multiyear average of the NHC strength (~~measure~~ metric (3)); $\langle \psi^{max} \rangle_p$ denotes the vertically averaged ψ^{max} between 200 hPa and 900 hPa (~~measure~~ metric (4), Eq. **??**); and ψ_{NHC} denotes the ~~measure~~ metric of the ~~average~~ spatially-averaged HC strength (~~measure~~ metric (7), Eq. ~~??~~??). Analogous notations are used for the ~~stream function~~ stream-function minimum for the SHC in (b). The following ~~measures~~ metrics do not distinguish between the two Hadley cells, but describe the Hadley circulation as a whole (their time-series are thus the same for NHC in (a) and SHC in (b)): $[\Phi]^{max}(p)$ denotes the maximum of the zonal-mean velocity potential at different pressure levels (~~measure~~ metric (5), ~~orange~~ violet colours); $[\omega]^{min}(p)$ denotes the minimum of the zonal-mean vertical velocity (~~measure~~ metric (6), ~~violet~~ orange colours); v_E denotes effective wind for the lower-tropospheric water vapour transport (metric (8), blue colour); and I_M denotes the normal-modes-based ~~index~~ metric of the Hadley circulation (~~measure~~ metric (~~8~~9), red colour).

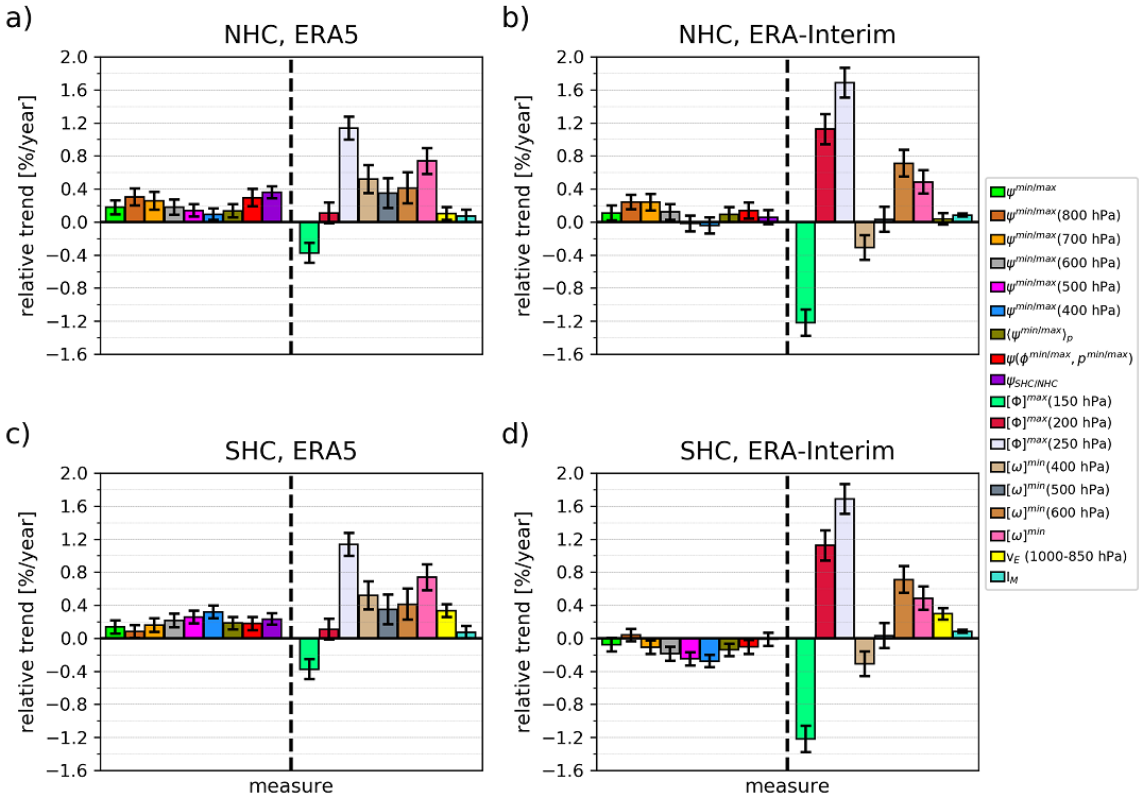

Figure 4. Annual-mean HC strength trends normalized by the climatological-mean values of the HC strength in the NH (a,b) and SH (c,d) in ERA5 (a,c) and ERA-Interim (b,d) reanalyses between 1979-2018 for different ~~measures~~ metrics of HC strength defined in Section 2.3. Different ~~measures~~ metrics of the HC strength are shown in the legend, e.g. for the NHC: ψ^{max} denotes the annual-mean stream-function maximum (metric (1)); ψ^{max} at 400 hPa, ~~450~~ 500 hPa, ~~..~~etc. denotes the annual-mean ~~stream function~~ stream-function maximum at respective pressure level (~~measure~~ metric (2)); ~~ψ^{max} denotes the annual-mean stream function maximum (measure (1));~~ $\psi(\varphi^{max}, p^{max})$ denotes that the trends are measured at the point of the maximum stream function in a multiyear average of the NHC strength (~~measure~~ metric (3)); $\langle \psi^{max}(t) \rangle_p$ denotes the vertically averaged $\psi^{max}(t)$ between 200 hPa and 900 hPa (Eq. 2) (~~measure~~ metric (4)); and ψ_{NHC} denotes the ~~measure~~ metric of ~~average~~ spatially-averaged HC strength (Eq. 3) (~~measure~~ metric (7)). Analogous notations are used for the ~~stream function~~ stream-function minimum for the SHC. The following ~~measures~~ metrics do not distinguish between the two Hadley cells, but describe the Hadley circulation as a whole (their results are the same for the NHC and the SHC, and are separated by the vertical black dashed line): $[\Phi]^{max}$ denotes the maximum of the zonal-mean velocity potential (~~measure~~ metric (5)), $[\omega]^{min}$ denotes the minimum of the zonal-mean vertical velocity (~~measure~~ metric (6)), v_E denotes effective wind for the lower-tropospheric water vapour transport (metric (8)) and I_M denotes the ~~normal-modes based index~~ normal-modes-based metric of the Hadley circulation (~~measure~~ metric (~~8~~9)). Note that positive values in all panels indicate strengthening of the NHC and SHC. Black error bars indicate standard error of the trend estimates.

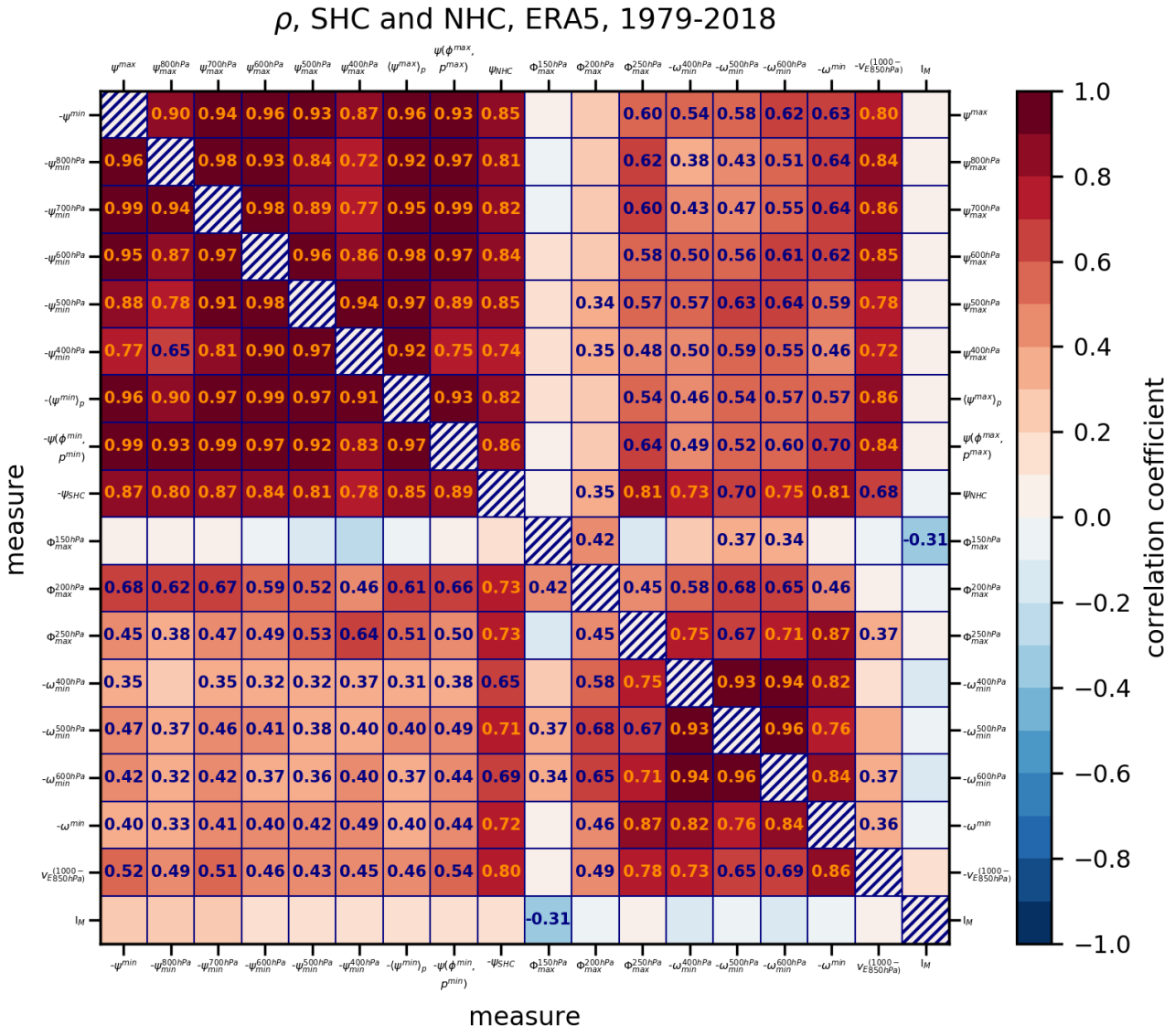

Figure 5. Correlations of time-series, derived from different ~~measures~~ metrics of the Hadley cell strength, described in Section ??, for 1979-2018 period in ERA5 reanalysis. The correlations for the northern Hadley cell are shown in the upper right part of the matrix, whereas the southern Hadley cell correlations are represented in the lower-left part. Time-series of $[\omega(p)]^{min}$ are multiplied by (-1) so that more positive values correspond to HC strengthening. Similarly, the time-series of the stream-function ~~based measures~~ metrics ψ_{min} are also multiplied by (-1) so that more positive values correspond to HC strengthening. Only correlations exceeding 95% significance threshold are shown.

Appendix A

MODES software (**?**) is used to perform scale- and circulation-type-dependent decomposition of the 3D dynamical fields: the zonal wind u, meridional wind v and modified geopotential $h = P/g$ with $P = \Phi + RT_0 \ln p_s$. Here, Φ represents the geopotential, R is the gas constant, $T_0(p)$ is globally-averaged temperature on a certain pressure level. The input data vector $[u, v, h]^T$ is decomposed using separable series of M orthogonal vertical structure functions $G_m(p)$ and series of horizontal structure functions (Hough harmonics) $\mathbf{H}_n^k(\lambda, \varphi; m)$, which consist of $2K + 1$ zonal waves and R meridional waves:

$$\begin{bmatrix} u(\lambda,\phi,p) \\ v(\lambda,\phi,p) \\ h(\lambda,\phi,p) \end{bmatrix} = \sum_{m=1}^{M} G_m(p)\,\mathbf{S}_m \sum_{n=1}^{R} \sum_{k=-K}^{K} \chi_{knm} \underbrace{\Theta_n^k(\varphi; m)\, e^{ik\lambda}}_{\mathbf{H}_n^k(\lambda,\varphi;m)}, \tag{A1}$$

where $\mathbf{S}_m = \mathrm{diag}(\sqrt{gD_m}, \sqrt{gD_m}, D_m)$ is a diagonal matrix, g is gravitatonal acceleration. D_m is an equivalent depth of the vertical mode m and couples the vertical and horizontal structure functions. χ_{knm} are the spectral Hough coefficients. $\Theta_n^k(\varphi; m)$ is meridional vector function consisting of multivariately related components $[U_n^k, -iV_n^k, Z_n^k]^T(\varphi; m)$. For every vertical mode m, the system of horizontal structure equations applies

$$\begin{aligned} &\frac{\partial u}{\partial t} - 2\Omega v \sin\varphi + \frac{g}{R\cos\varphi}\frac{\partial h}{\partial \lambda} = 0 \\ &\frac{\partial v}{\partial t} + 2\Omega u \sin\varphi + \frac{g}{R}\frac{\partial h}{\partial \varphi} = 0 \\ &\frac{\partial h}{\partial t} + D_m \nabla \cdot \mathbf{v} = 0. \end{aligned} \tag{A2}$$

The equations can be made dimensionless by taking $\widetilde{u} = u'/\sqrt{gD_m}$, $\widetilde{v} = v'/\sqrt{gD_m}$, $\widetilde{h} = h'/D_m$ and $\widetilde{t} = 2\Omega t$, so that

$$\frac{\partial}{\partial \widetilde{t}}\mathbf{W}_m + \mathbf{L}\mathbf{W}_m = \mathbf{0}, \tag{A3}$$

where $\mathbf{W}_m = [\widetilde{u}, \widetilde{v}, \widetilde{h}]^T$ and $\mathbf{L}$ is the linear differential matrix operator

$$\mathbf{L} = \begin{bmatrix} 0 & -\sin\varphi & \frac{\gamma}{\cos\varphi}\frac{\partial}{\partial\lambda} \\ \sin\varphi & 0 & \gamma\frac{\partial}{\partial\varphi} \\ \frac{\gamma}{\cos\varphi}\frac{\partial}{\partial\lambda} & \frac{\gamma}{\cos\varphi}\frac{\partial}{\partial\varphi}(\cos\varphi(\cdot)) & 0 \end{bmatrix}. \tag{A4}$$

γ is a dimensionless parameter defined as the ratio of shallow-water gravity wave speed and twice the rotation speed of Earth, $\gamma = \sqrt{gD_m}/(2R\Omega)$. The third equation in system (**??**) now becomes

$$\frac{\partial}{\partial \widetilde{t}}\widetilde{h}_m + \frac{\sqrt{gD_m}}{2\Omega}\left(\nabla \cdot \widetilde{\mathbf{v}}_m\right) = 0, \tag{A5}$$

The solution ansatz can be expressed by assuming separability of time-dependent and space-dependent solutions, i.e.

$$\mathbf{W}_m(\lambda, \phi, \widetilde{t}) = \mathbf{H}_n^k(\lambda, \phi; m) e^{-i\widetilde{\sigma}_{knm}\widetilde{t}}, \tag{A6}$$

where $\widetilde{\sigma}_{knm}$ is dimensionless frequency, and $\mathbf{H}_n^k(\lambda, \varphi; m)$ are the associated horizontal structure functions, which are used in the expansion (**??**).

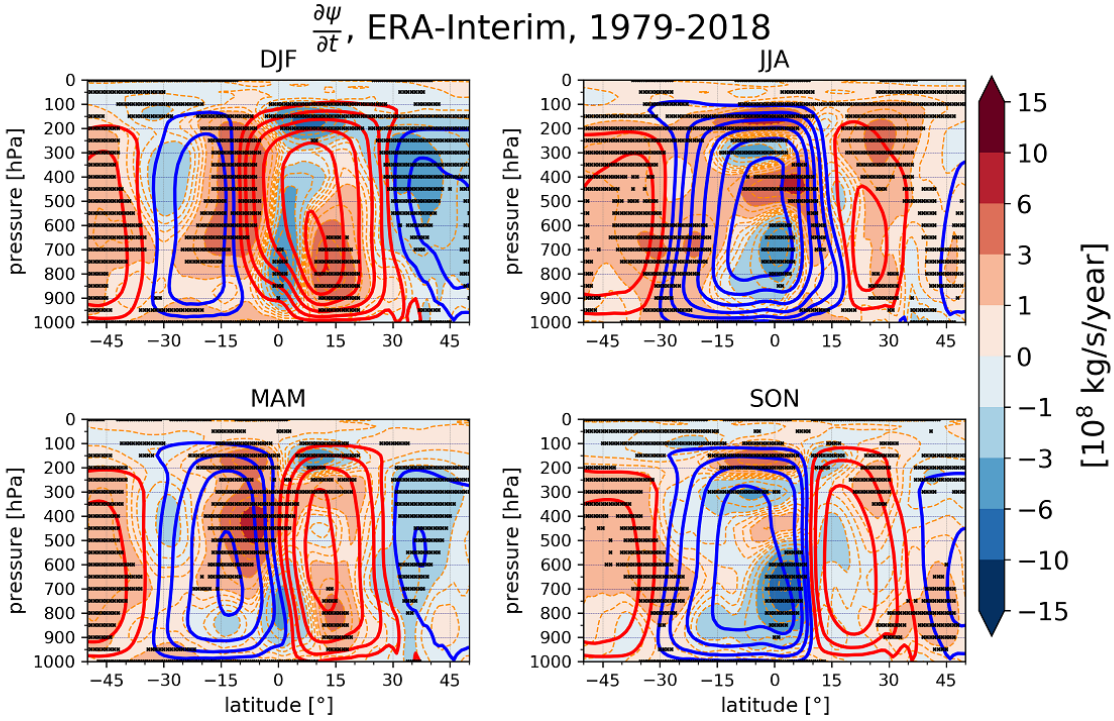

Figure A1. As in Fig. ????, but for the ERA-Interim reanalysis.

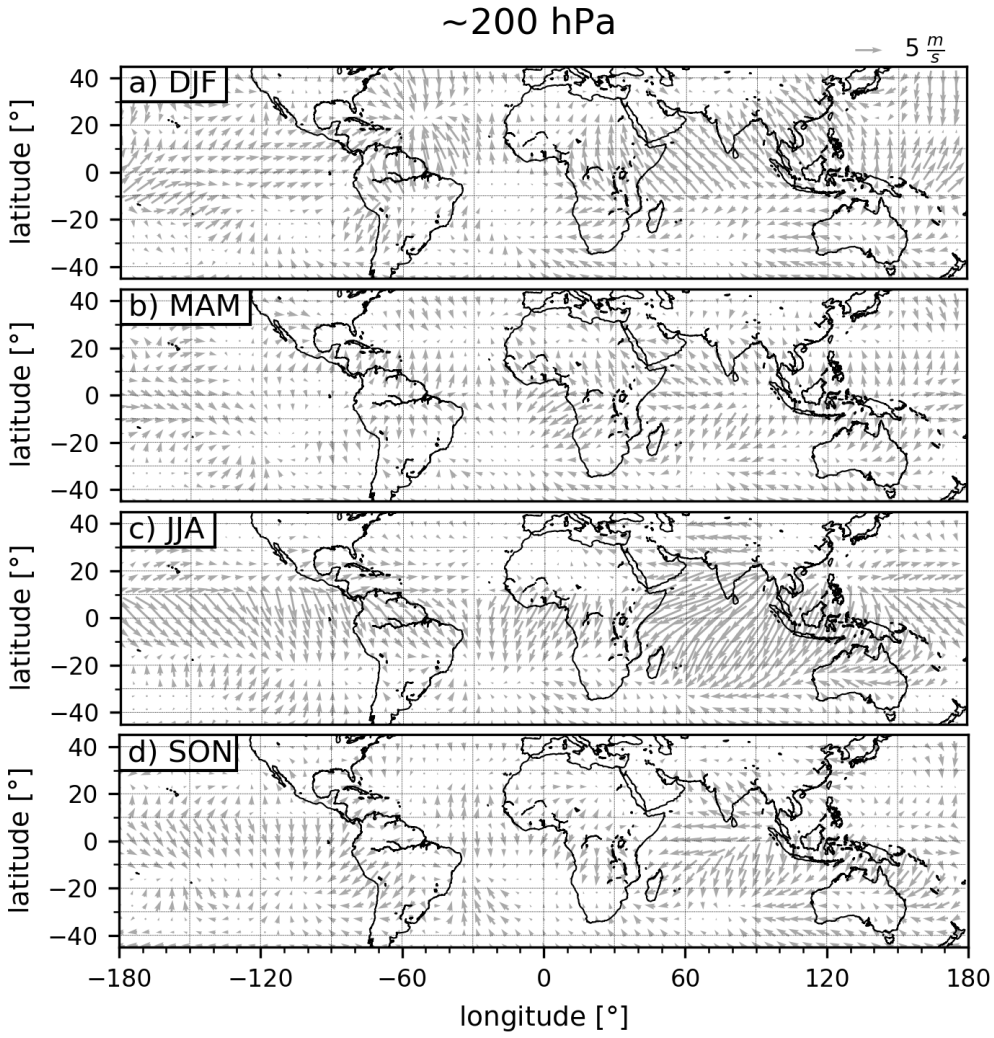

Figure A2. Horizontal winds for unbalanced circulation; in different seasons on 200 hPa pressure level. Wind intensity is shown by the length of the wind vectors.

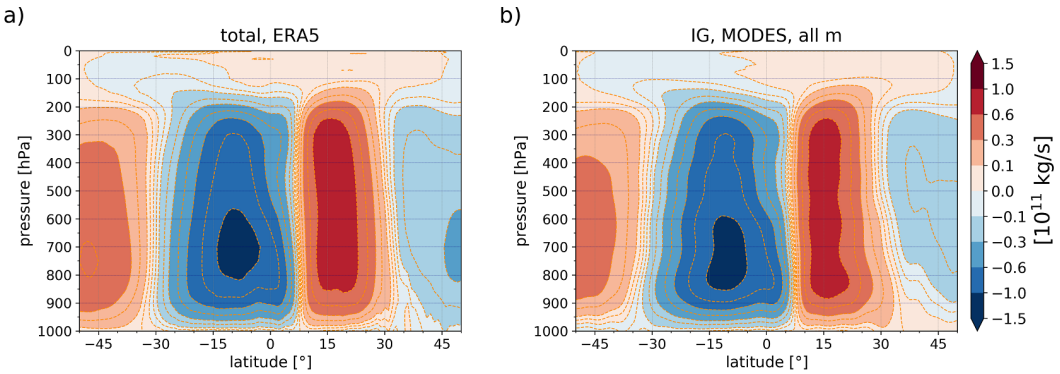

Figure A3. The 2018 mean Hadley Circulation (red and blue contours) in ERA5 reanalysis computed from (a) total fields of zonal-mean meridional wind and (b) unbalanced (inertia-gravity) fields. Contours indicate values of stream function ψ.

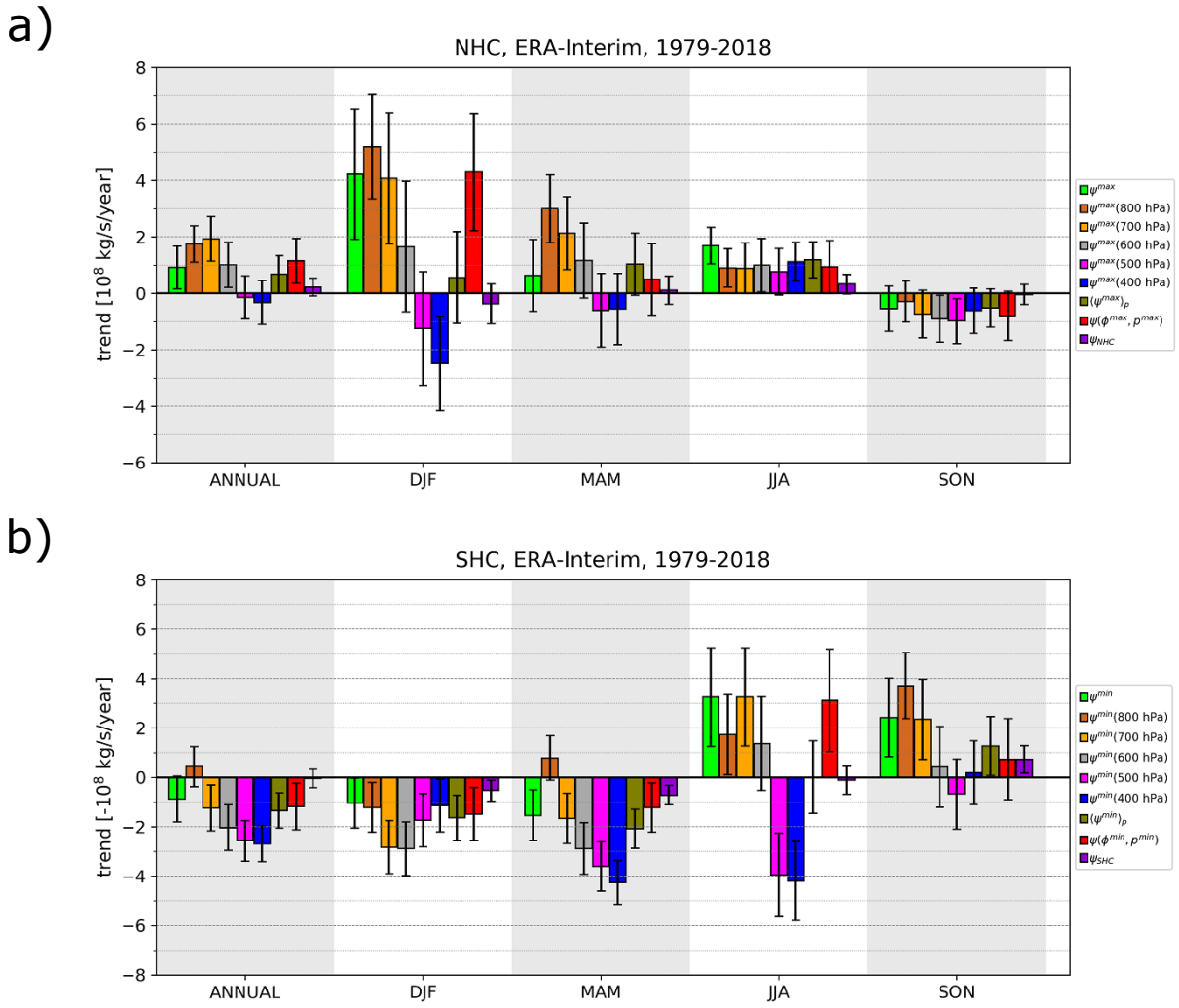

Figure A4. As in Fig. **??**, but for the ERA-Interim reanalysis.

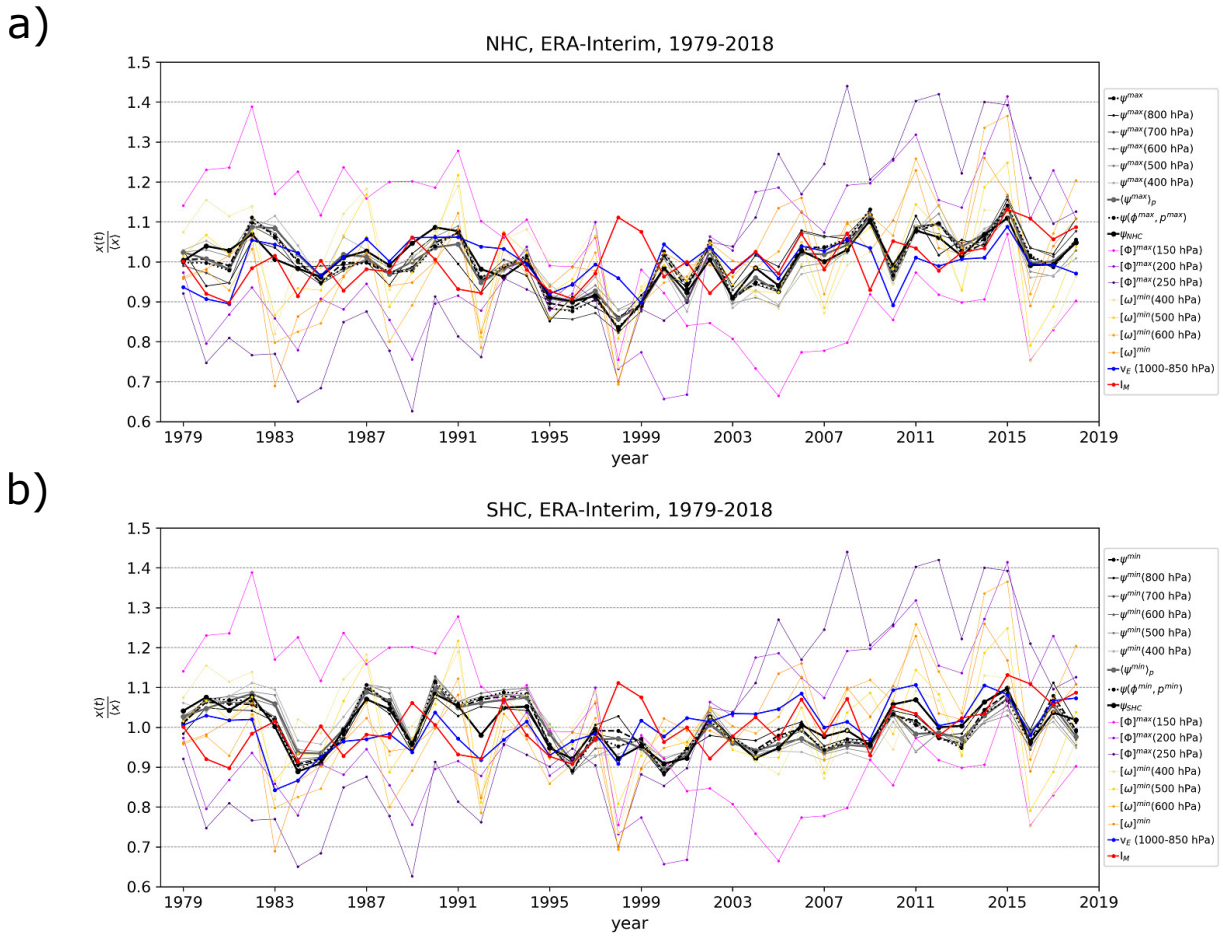

Figure A5. As in Fig. **??**, but for the ERA-Interim reanalysis.

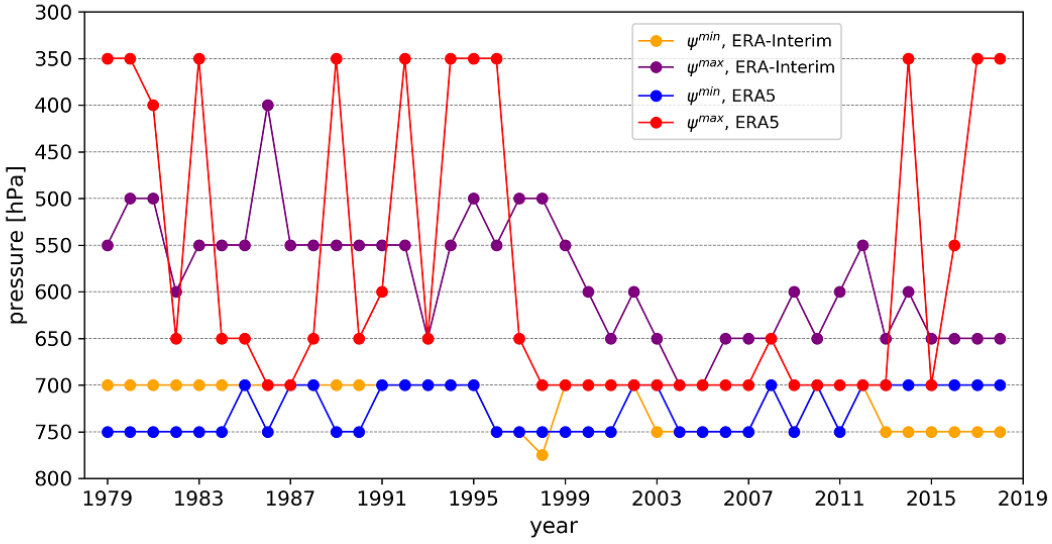

Figure A6. Level of maximum/minimum stream function in annual-mean Hadley circulation between 1979-2018 in ERA5 and ERA-Interim reanalyses.

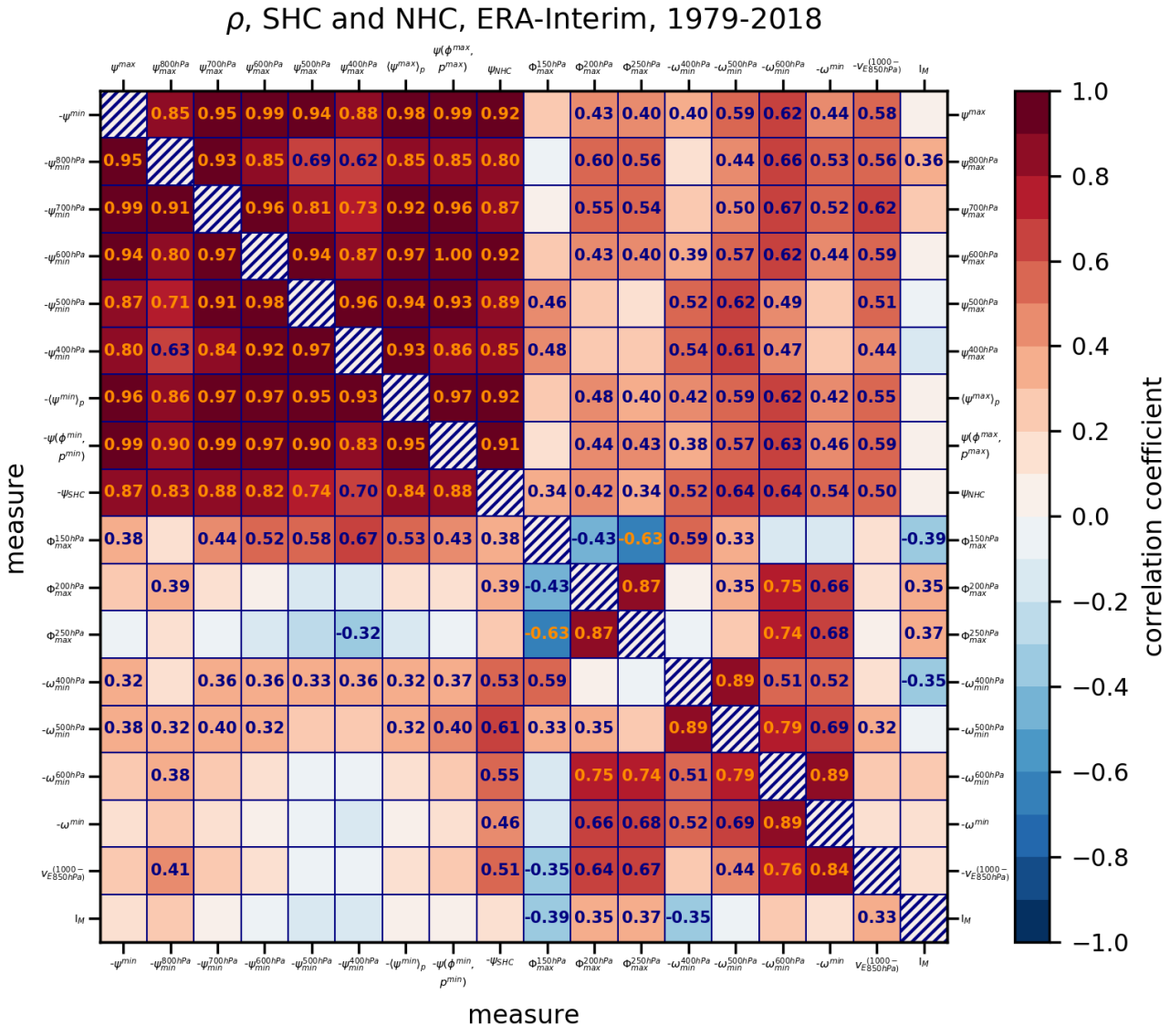

Figure A7. As in Fig. **??**, but for ERA-Interim.

Table A1. As in Table **??**, but for ERA-Interim.

NHC ~~measure~~ metric	trend (± unc.) [%/yr]	SHC ~~measure~~ metric	trend (± unc.) [%/yr]	HC ~~measure~~ metric	trend (±
ψ^{max}	0.109 (± 0.091)	ψ^{min}	-0.077 (± 0.082)	$[\Phi]^{max}$ (150 hPa)	-1.22
ψ^{max} (800 hPa)	0.240 (± 0.088)	ψ^{min} (800 hPa)	0.039 (± 0.075)	$[\Phi]^{max}$ (200 hPa)	1.12
ψ^{max} (750 hPa)	0.259 (± 0.094)	ψ^{min} (750 hPa)	-0.036 (± 0.079)	$[\Phi]^{max}$ (250 hPa)	1.68
ψ^{max} (700 hPa)	0.239 (± 0.098)	ψ^{min} (700 hPa)	-0.109 (± 0.082)	$[\omega]^{min}$ (400 hPa)	-0.31
ψ^{max} (650 hPa)	0.191 (± 0.098)	ψ^{min} (650 hPa)	-0.161 (± 0.084)	$[\omega]^{min}$ (500 hPa)	0.03
ψ^{max} (600 hPa)	0.121 (± 0.096)	ψ^{min} (600 hPa)	-0.188 (± 0.084)	$[\omega]^{min}$ (600 hPa)	0.71
ψ^{max} (550 hPa)	0.043 (± 0.094)	ψ^{min} (550 hPa)	-0.212 (± 0.082)	$[\omega]^{min}$	0.48
ψ^{max} (500 hPa)	-0.018 (± 0.093)	ψ^{min} (500 hPa)	-0.248 (± 0.080)	I_M	~~0.276~~ 0.084 (±
ψ^{max} (450 hPa)	-0.055 (± 0.095)	ψ^{min} (450 hPa)	-0.287 (± 0.077)		
ψ^{max} (400 hPa)	-0.041 (± 0.098)	ψ^{min} (400 hPa)	-0.278 (± 0.075)		
$\psi(\varphi^{max}, p^{max})$	0.138 (± 0.096)	$\psi(\varphi^{min}, p^{min})$	-0.105 (± 0.084)		
$\langle\psi^{max}\rangle_p$	0.092 (± 0.090)	$\langle\psi^{min}\rangle_p$	-0.141 (± 0.074)		
~~ψ^{NHC}~~ ψ_{NHC}	~~0.054~~ 0.058 (± 0.086)	ψ_{SHC}	~~-0.009~~ -0.012 (± ~~0.079~~0.080)		
v_E^{NHC} (1000-850 hPa)	0.038 (± 0.071)	v_E^{SHC} (1000-850 hPa)	0.295 (± 0.069)		

Author contributions. MP performed numerical analysis and generated all figures. ŽZ devised the research, performed the modal analysis and wrote the first draft of the manuscript. NŽ oversaw modal analysis. LB and NŽ provided additional insight and helped improve the manuscript for the final version.

Competing interests. The authors declare that they have no conflict of interest.

Acknowledgements. We thank two anonymous reviewers for their comprehensive reviews. MP is supported by ARRS Programme P1-0188. ŽZ is funded by the Slovenian Research Agency project J1-9431 and is also supported by ARRS Programme P1-0188. LB is supported by Trond Mohn Foundation (project BCPU, grant number BFS2018TMT01). Research of N. Ž. contributes to the Cluster of Excellence 405 "CLICCSClimate, Climatic Change, and Society" of the Center for Earth System Research and Sustainability (CEN) of Universität Hamburg.